Barrel Cortex Critical Period Plasticity Is Independent of Changes in NMDA Receptor Subunit Composition

Hui-Chen Lu, Ernesto Gonzalez,
and Michael C. Crair[1]
Division of Neuroscience and
Program in Developmental Biology
One Baylor Plaza, S-603
Baylor College of Medicine
Houston, Texas 77030

Summary

The regulation of NMDA receptor (NMDAR) subunit composition and expression during development is thought to control the process of thalamocortical afferent innervation, segregation, and plasticity. Thalamocortical synaptic plasticity in the mouse is dependent on NMDARs containing the NR2B subunit, which are the dominant form during the "critical period" window for plasticity. Near the end of the critical period there is a gradual increase in the contribution of NR2A subunits that happens in parallel to changes in NMDAR-mediated current kinetics. However, no extension of the critical period occurs in NR2A knockout mice, despite the fact that NMDA subunit composition and current kinetics remain immature past the end of the critical period. These data suggest that regulation of NMDAR subunit composition is not essential for closing the critical period plasticity window in mouse somatosensory barrel cortex.

Introduction

In the mammalian brain, neural circuits that receive input relayed from the sensory periphery are often organized into regular neuronal arrays or maps. A characteristic property of these brain maps is that groups of neighboring neurons respond to similar features of stimuli presented to the sensory periphery. Well-known examples are the maps of body-surface in somatosensory cortex (the so called "homunculus" in humans) and the representation of eye preference (ocular dominance) in visual cortex (Hubel and Wiesel, 1977; Mountcastle, 1957). In the rodent, large hairs on the snout ("whiskers") are arranged in a regular pattern of rows and arcs. This specific pattern of facial whiskers is recapitulated throughout the somatosensory trigeminal pathway in the form of clusters of neurons that respond preferentially to stimulation of a single whisker. The neuronal modules in the cortical map of facial whiskers are called "barrels," which due to their easy visualization and manipulation have become an important model system for studying the mechanisms underlying cortical map development and plasticity (Woolsey, 1990).

One feature of sensory maps is their malleability in the face of a changing environment, such that altered patterns of experience lead to corresponding changes in map structure. For instance, Hubel and Wiesel (1963)

demonstrated that depriving one eye of visual experience (monocular deprivation) during development causes the cortical map for eye preference to shift in the favor of the open eye. This ocular dominance plasticity can only be induced if the deprivation is performed during a so called "critical period" of map development. The rodent somatosensory barrel cortex exhibits a similar kind of developmental map plasticity. If a row of whiskers is removed (cauterized) during a critical period in the development of the cortex, barrels serving the deprived whiskers shrink while neighboring barrels from the intact whiskers expand. The degree of "filling in" or plasticity becomes progressively smaller the later in development that the deprivation is started. By around postnatal day 6 or 7 (P6–P7), whisker cautery has little obvious effect on barrel cytoarchitectonic structure (Woolsey, 1990), marking the end of the critical period for barrel development.

The N-methyl-D-aspartate (NMDA) subtype of the glutamate receptor (GluR), which is a voltage- and ligand-gated channel permissive to Ca^{2+} ions, is thought to play an important role in the development and plasticity of barrels in rodent somatosensory cortex. Mice with a null mutation in the gene for either the NR1 or NR2B subunit of the NMDA receptor (also called GluRζ and GluRε2, respectively), lack whisker-related somatotopic maps in the entire trigeminal pathway, including the brainstem and thalamus (Iwasato et al., 1997; Kutsuwada et al., 1996; Li et al., 1994). Mice with a mutation in the NR1 subunit that is restricted to the cortex, lack cytoarchitectonic barrels only in the cortex (Iwasato et al., 2000). In addition, barrel map plasticity (Iwasato et al., 1997; Schlaggar et al., 1993; Rema et al., 1998; Fox et al., 1996) induced by neonatal whisker cauterization is reduced when NMDA receptor (NMDAR)-mediated synaptic activity in the cortex is blocked by application of the NMDAR-specific antagonist, APV (D(−)-2-Amino-5-phosphonopentanoic acid). Collectively, these data suggest that many aspects of the development and plasticity of a whisker-related pattern in rodent somatosensory cortex are mediated by NMDAR-dependent neuronal activity, as is also known to be the case for ocular dominance column plasticity in the visual cortex (Bear et al., 1990; Kleinschmidt et al., 1987; Roberts et al., 1998).

NMDARs are multimeric proteins composed of at least one NR1 subunit and up to four subunits of the NR2 family (Schoepfer et al., 1994, Sheng et al., 1994). The NR2 family itself contains at least four members, NR2A–NR2D (also called GluRε1–GluRε4). Expression of the different NR2 subunits is regulated during development so that the NR2B subunit is already highly expressed in the embryonic cortical plate, while the NR2A subunit begins to be expressed in the cortex a few days after birth. The NR2C and NR2D subunits appear never to have a very high level of expression in the cortex (Watanabe et al., 1992; Monyer et al., 1994; Sheng et al., 1994; Wang et al., 1995; Zhong et al., 1995; Cao et al., 2000a, 2000b; Kirson and Yaari, 1996; Sun et al., 2000). Several studies have demonstrated that the current through immature NMDARs composed of only the NR1 and NR2B

subunits is very long lasting (Flint et al., 1997; Vicini et al., 1998; Tovar and Westbrook, 1999; Tovar et al., 2000; Steigerwald et al., 2000). These studies also suggest that the presence of the NR2A subunit in more mature NMDARs may accelerate the decay of the NMDAR current.

The subunit composition of NMDARs is differentially regulated by neuronal activity (Hoffmann et al., 2000; Vallano et al., 1996) and sensory experience (Quinlan et al., 1999a, 1999b; Nase et al., 1999; Ramoa and Prusky, 1997; Carmignoto and Vicini, 1992; Philpot et al., 2001), suggesting that changes in NMDAR subunit composition might put synapses into a nonpermissive plasticity state. These developmental changes could lead to a reduction in synaptic plasticity, perhaps as a result of a decreased ability of the synapse to temporally integrate calcium influx due to faster NMDAR synaptic current decay times (Scheetz and Constantine-Paton, 1994; Hestrin, 1992; Carmignoto and Vicini, 1992; Shi et al., 2000; Crair and Malenka, 1995; Kirson and Yaari, 1996; Tang et al., 1999; Barth and Malenka, 2001). This has led to the hypothesis that the developmental regulation of the NMDAR, presumably through subunit composition, may serve as a mechanism for experience-dependent modulation of both synaptic plasticity and map plasticity in the brain (for reviews, see Crair, 1999; Fox and Zahs, 1994; Katz and Shatz, 1996; Singer, 1995).

Several labs have explored the properties of functional thalamocortical synapse development in somatosensory cortex (S1) of the rodent using an acute thalamocortical brain slice preparation (Agmon and Connors, 1991; Agmon and O'Dowd, 1992; Crair and Malenka, 1995; Gil et al., 1999; Isaac et al., 1997; Kidd and Isaac, 1999; Barth and Malenka, 2001). One focus of these investigations is on mechanisms of thalamocortical synapse maturation that may play a role in barrel map development and plasticity. NMDAR-dependent synaptic plasticity at the thalamocortical synapse in the rat parallels the critical period for barrel plasticity so that LTP and LTD at the thalamocortical synapse is easy to induce during the critical period, and difficult thereafter (Crair and Malenka, 1995; Feldman et al., 1998; Isaac et al., 1997). In this report, we present evidence for a developmental window for synaptic plasticity at the thalamocortical synapse in mouse barrel cortex that corresponds to the critical period for anatomical and functional plasticity, as was found in the rat. We also show that thalamocortical LTP is blocked by the NR2B subunit-specific NMDAR antagonist, ifenprodil. We further demonstrate that the subunit composition of the NMDAR at thalamocortical synapses is developmentally regulated, changing from largely NR2B during the critical period to mixed NR2A/2B near the end of the critical period. The developmental transition of the NR2 subunit parallels the decrease in the decay time constant of NMDAR current at thalamocortical synapses and the end of the thalamocortical synaptic plasticity window. Using NR2A loss-of-function ("knockout") mutant mice, we demonstrate that expression of the NR2A subunit is required for the developmental regulation of NMDA current kinetics at thalamocortical synapses. Surprisingly, however, the critical period for thalamocortical synaptic plasticity and barrel map plasticity remains unchanged in NR2A knockout mice. This suggests that regulation of NMDAR subunit composition, as well as the associated change in NMDA current kinetics, is not required to close the

critical period window for anatomical and synaptic plasticity in barrel cortex.

Results

NR2B-Dependent Critical Period Synaptic Plasticity in the Mouse

Barrel maps form and are plastic during the first week after birth in both the rat and the mouse. Using whole-cell voltage clamp recording techniques in the mouse, we confirmed the critical period correspondence between synaptic plasticity (LTP) and barrel map plasticity previously demonstrated in the rat (Crair and Malenka, 1995). Thalamocortical LTP was induced with a standard "pairing protocol" (Gustafsson et al., 1987; Malenka and Nicoll, 1993; Bi and Poo, 2001) in which the thalamus is stimulated 100 times at 1 Hz while simultaneously depolarizing layer IV barrel neurons to −10 mV (Figure 1). Pairing is a strong LTP-inducing protocol that enforces the coincident activation of pre- and postsynaptic neurons without regard to network activity. Robust pairing-induced LTP is easy to induce at thalamocortical synapses within a week of birth (71% ± 15% LTP at P3–P4, n = 10; 56% ± 11% LTP at P5–P7, n = 6) (Figures 1A–1D), but difficult thereafter (−1% ± 9% LTP at P9–P11, n = 7, p < 0.01 for the difference between P3–P4 or P5–P7 and P9–P11). This matches the time when LTP could be induced at thalamocortical synapses in the rat (Crair and Malenka, 1995) and corresponds to the critical period for cytoarchitectonic plasticity in the mouse and rat (Woolsey, 1990) and to the time of maximal plasticity measured in layer IV of rat barrel cortex in vivo (Fox, 1992).

Thalamocortical LTP may be easy to elicit in young mice but difficult thereafter because of a difference in the character or quantity of NMDARs at the synapse. We checked whether the NR2B subunit, which is the most abundantly expressed subunit in neonates, is necessary for thalamocortical synaptic plasticity. We found that thalamocortical LTP was blocked by 3 μM ifenprodil (mean LTP −1% ± 5%, n = 8; 65% ± 13% in n = 12 interleaved control cells; all neurons P3–P5, p < 0.05) (Figures 1E–1H); the standard concentration used to selectively antagonize NR2B-mediated NMDA currents (Williams, 1993; Tovar and Westbrook, 1999). Thus, critical period thalamocortical LTP in the mouse is not only NMDAR dependent, but specifically requires the contribution of NMDARs containing the NR2B subunit.

AMPA/NMDA Currents at Thalamocortical Synapses

The thalamocortical synapse is composed of a mix of AMPA (α-amino-3-hydroxyl-5-methyl-4-isoxazolepropionate), Kainate, and NMDA receptors whose functional expression is developmentally regulated. We investigated the relative contribution of AMPAR and NMDAR currents to thalamocortical synaptic response in the developing mouse. Large NMDAR currents were observed in mice less than one week old (P3–P6, median AMPAR/NMDAR is 0.27 ± 0.12; n = 17) (Figures 2A and 2B), and the contribution of AMPARs increased significantly through the first postnatal week (P8–P11, median AMPAR/NMDAR is 1.36 ± 0.58; n = 14) (Figures 2A and 2B). The observed increase (p < 0.01, Mann-Whitney rank sum test) in the AMPAR/NMDAR ratio could be due
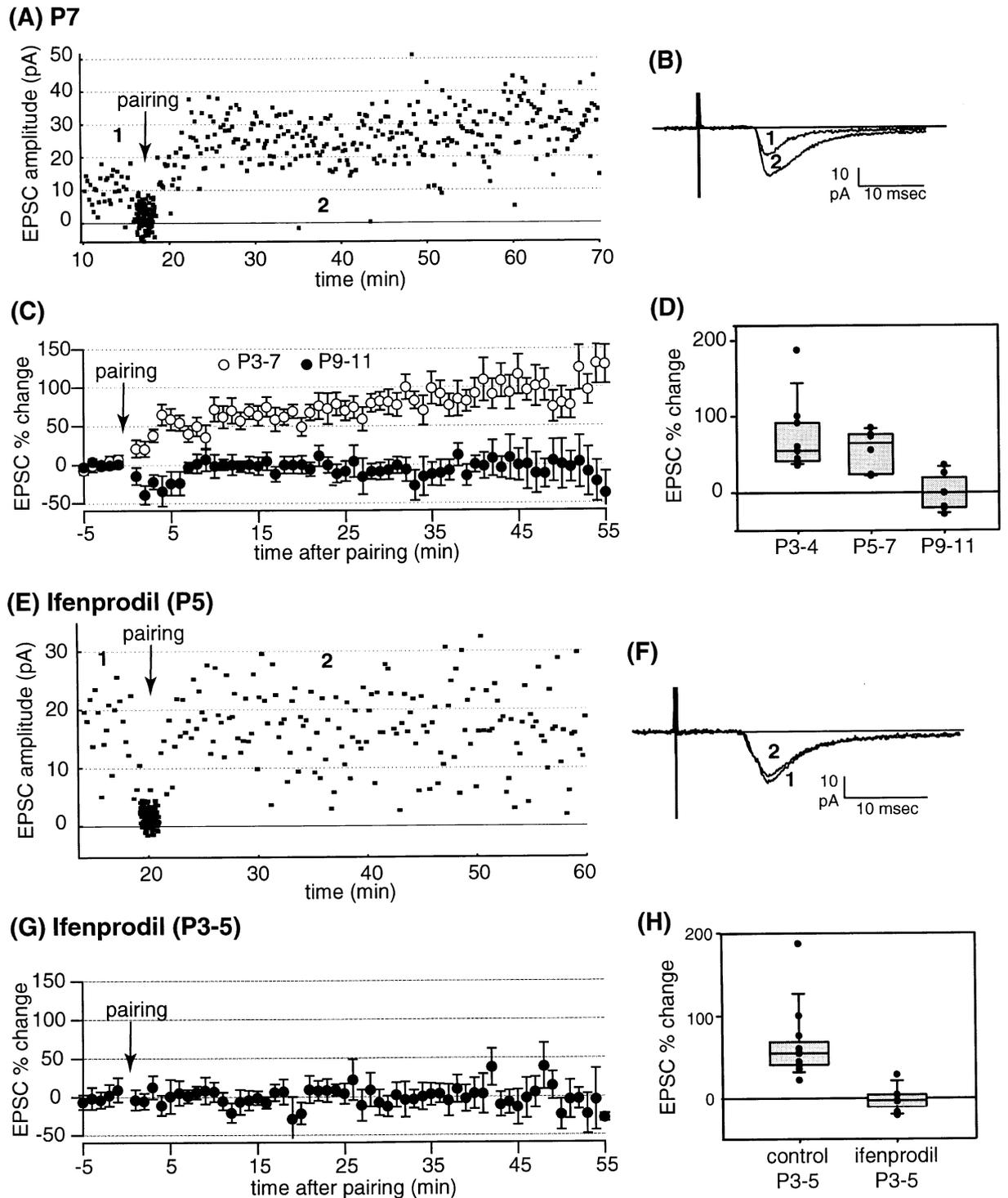
Figure 1. Critical Period for NR2B-Dependent Thalamocortical LTP in the Mouse

(A) Example of LTP at the thalamocortical synapse (P7) induced by pairing (at arrow) postsynaptic depolarization (-10 mV) with presynaptic stimulation (1 Hz for 100 s). (B) Example traces (average of 30 sweeps) before (1) and after (2) LTP, showing an increase in the amplitude of the EPSC as a result of pairing. (C) Summary graph from P3–P7 (n = 16) and P9–P11 (n = 7) mice. (D) Significant LTP can be induced during the first week after birth, (P3–P4, 71 $\pm$ 15%, n = 10; P5–P7, 56 $\pm$ 11%, n = 6), but not thereafter (P9–P11, $-1\% \pm 9\%$; n = 7; p < 0.01). (E) The NR2B specific antagonist ifenprodil (3 μM) blocks thalamocortical LTP. Ifenprodil was present in the perfusate for more than 30 min prior to pairing and remains in the perfusate during the entire recording. (F) Example traces before (1) and after (2) pairing, showing no change in the EPSC amplitude (average of 10 sweeps). (G) Summary of eight cells (P3–P5) similarly treated with ifenprodil. (H) Summary of EPSC % change induced by pairing in twelve control cells (P3–P5; 65% $\pm$ 13%) that were interleaved with eight ifenprodil treated neurons (P3–P5; 1% $\pm$ 5%). Significantly less LTP is induced in the presence of ifenprodil (p < 0.01), and LTP is blocked in seven out of eight cells. Box plots show the median, 10th, 25th, 75th, and 90th percentiles as vertical boxes with error bars.

to a developmental increase in AMPARs, a decrease in NMDARs, or both. In any case, the AMPAR component of the thalamocortical response becomes relatively large after the first week of postnatal development in the mouse. This result is consistent with the suggestion that AMPARs are gradually incorporated into the thalamocortical synapse during development (Crair and Malenka, 1995), potentially by adding AMPARs to synapses that were previously composed of only NMDARs ("silent synapses") (Isaac et al., 1997).

Increased NR2A during Thalamocortical Synapse Development

In addition to a change in the relative contribution of the NMDA and AMPA receptors, the kinetics of the NMDAR response changes over the course of development. During the first postnatal week the decay of the NMDAR currents was generally slow (Figures 2C and 2E), with a mean weighted time constant of 307 ± 35 ms for P3–P4 mice (n = 8) (see Experimental Procedures) and 283 ± 39 ms for P5–P6 mice (n = 10). Thereafter (P9–P11; n = 14), the NMDAR currents decline significantly faster, with a time constant of 183 ± 22 ms (p < 0.01).

We used the NR2B-selective antagonist, ifenprodil, to estimate the contribution of NR2B containing NMDARs to the entire NMDAR EPSC at thalamocortical synapses during critical period development. We found that the relative contribution of NR2B currents gradually decreased over the first 7–10 days postnatal (Figures 2D and 2F). Most of the NMDAR current at P3–P4 was ifenprodil sensitive ($81\% \pm 3\%$, n = 9). There was a small but significant decrease in ifenprodil sensitivity already at P5–P6 ($67\% \pm 4\%$, n = 13; p < 0.05). For P9–P11 neurons, ifenprodil was even less effective at blocking the NMDAR-mediated EPSC ($32\% \pm 5\%$, n = 8; p < 0.01 for the difference between P9–P11 and either P3–P4 or P5–P6).

There is very little NR2C and NR2D expression in barrel cortex, so the increase in ifenprodil resistant currents likely reflects an increase in the fraction of NMDARs containing the NR2A subunit at thalamocortical synapses (Watanabe et al., 1992; Monyer et al., 1994; Wang et al., 1995; Zhong et al., 1995; Cao et al., 2000a; 2000b; Sun et al., 2000) (Western data not shown). Thus, NR2A-containing NMDARs begin to increase their contribution to thalamocortical synapses at P5–P6 and dominate by P9–P11. The observed correlation between the increase of NR2A subunit containing NMDARs, and the decrease of the NMDA current decay time suggests that NR2A incorporation into NMDARs modulates receptor kinetics.

NMDA Currents at Thalamocortical Synapses in NR2A Mutant Mice

Next, we tested the role of subunit composition on NMDAR current kinetics with loss-of-function mutant mice lacking NR2A subunits. NR2A homozygous mutant mice have grossly normal cortical and thalamic anatomy, including a normal barrel pattern, normal cortical lamina, and normal physiological response (input-output profiles, paired-pulse facilitation, time course of field potential response, resting membrane potential, and input resistance) (see Sakimura et al., 1995; data not shown), though they display learning and memory defi- cits as adults (Kiyama et al., 1998). NMDAR time constants at the thalamocortical synapse of homozygous ($NR2A^{-/-}$), heterozygous ($NR2A^{+/-}$), and wild-type ($NR2A^{+/+}$) littermates were examined in neonatal mice (between P4 and P11) while remaining blind to the genotype of the animal. This is the age range when the NR2A subunit normally begins to contribute to NMDAR currents at wild-type synapses (Figure 2). In P4–P7 mice, NR2A subunits make a modest contribution to NMDAR currents (Figure 2F), and NMDAR currents were correspondingly somewhat longer lasting (Figures 3A and 3B, gray histogram) in $NR2A^{-/-}$ mice (378 ± 43.0 ms; n = 10) relative to $NR2A^{+/+}$ controls (249 ± 22.6 ms; n = 12; p < 0.05). $NR2A^{+/-}$ mice fell midway between their $NR2A^{-/-}$ and $NR2A^{+/+}$ littermates (283 ± 44 ms; n = 8). At P8–P11, when NR2A subunits normally contribute significantly to NMDAR currents (Figure 2F), there is a dramatic difference in NMDAR kinetics (Figure 3B, white histogram) between $NR2A^{-/-}$ (331 ± 42 ms; n = 9) and both $NR2A^{+/-}$ (200 ± 15 ms; n = 12; p < 0.01) and $NR2A^{+/+}$ controls (160 ± 15 ms; n = 11; p < 0.01).

We also examined the sensitivity of NMDAR currents in the NR2A mutant mice to the NR2B specific antagonist ifenprodil. At P4–P7, when the contribution of NR2A subunits to the NMDA current is normally small (Figures 3C and 3D, gray histogram), there is no significant difference in the ifenprodil (3 μm) sensitivity between $NR2A^{-/-}$ ($68\% \pm 5\%$; n = 10), $NR2A^{+/-}$ ($52\% \pm 6\%$; n = 6), and $NR2A^{+/+}$ mice ($67\% \pm 8\%$; n = 11; p = 0.92). By P8–P11, however, $NR2A^{-/-}$ mice remain highly sensitive to ifenprodil (Figures 3C and 3D, white histogram, $54.2\% \pm 7.5\%$ response suppression; n = 7) while $NR2A^{+/+}$ mice become much less sensitive to ifenprodil, ($30\% \pm 8\%$; n = 6; p < 0.05 between $NR2A^{+/+}$ and $NR2A^{-/-}$), and $NR2A^{+/-}$ mice are somewhat less sensitive ($36\% \pm 7\%$; n = 7; p = 0.1 between $NR2A^{+/-}$ and $NR2A^{-/-}$), reflecting the increased contribution of NR2A subunits to NMDA currents at thalamocortical synapses at these ages.

Comparing the developmental time course of changes in ifenprodil sensitivity and NMDAR current kinetics (Figures 3E and 3F), it is apparent that faster kinetics and decreased ifenprodil sensitivity develop in parallel through the first 7–10 days after birth. In the $NR2A^{+/+}$ mice (Figure 3E), there is a gradual decrease in both the ifenprodil sensitivity (open white bars) and time constant (gray bars) between P4 and P11, though the ifenprodil sensitivity does decrease more quickly with age. In the $NR2A^{-/-}$ mice, there is no change in either the ifenprodil sensitivity (Figure 3F, gray bars) or weighted time constant (Figure 3F, open white bars) between P4 and P8, and a small but insignificant (p = 0.4) decrease in both by P11. The results for the $NR2A^{+/-}$ mice (Figures 3B and 3D) appear to fall midway between those for the $NR2A^{-/-}$ and $NR2A^{+/+}$ mice. This suggests that the observed change in NMDAR current kinetics with development relies on modification in the subunit structure of the NMDAR at the thalamocortical synapse.

Critical Period for Thalamocortical LTP Unchanged in $NR2A^{-/-}$ Mice

Previous work in the visual system has shown that NR2A subunit expression is modulated by visual experience during development (Quinlan et al., 1999a, 1999b; Nase
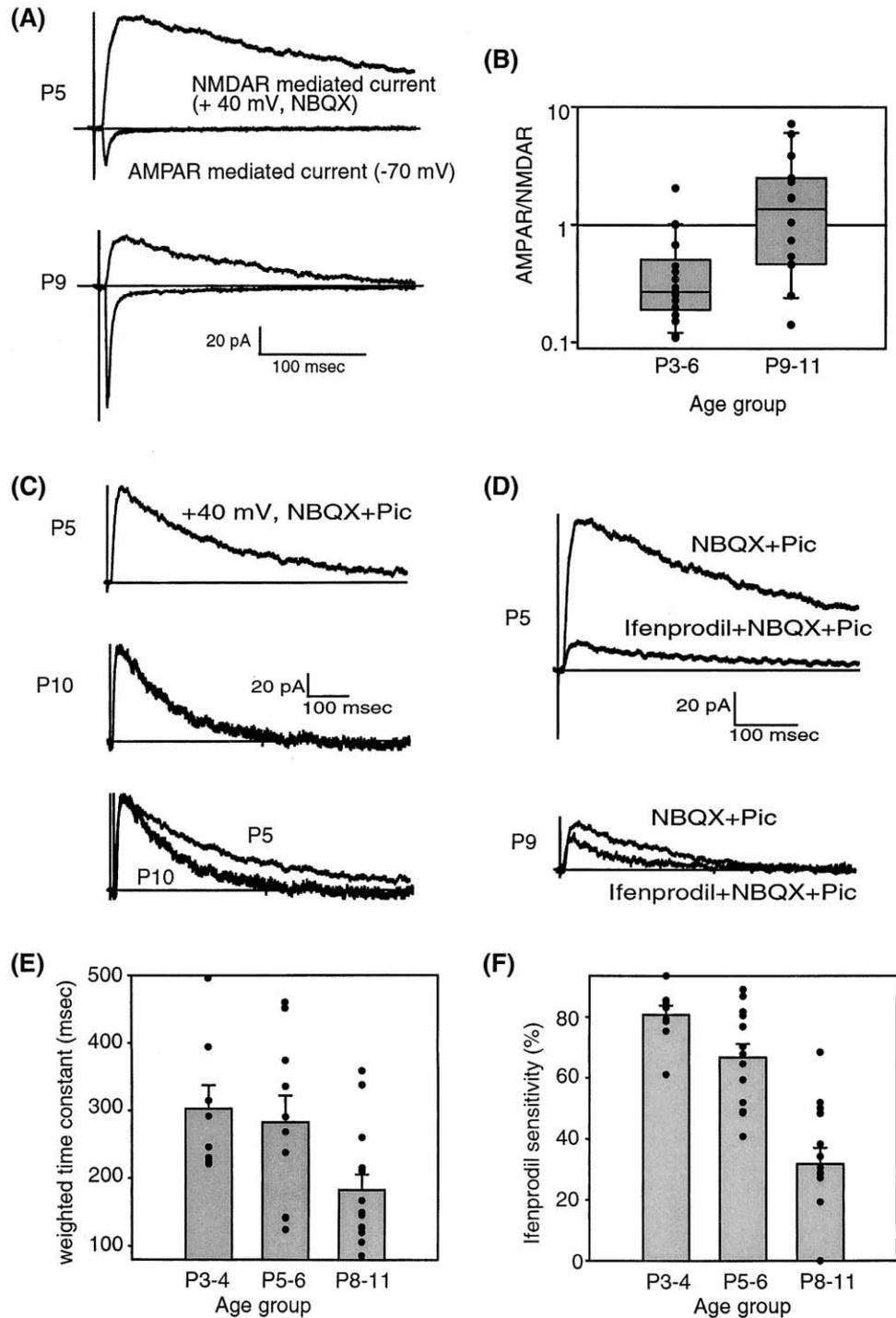
Figure 2. Developmental Changes in AMPA/NMDA Currents and NMDAR Subunit Composition at the Thalamocortical Synapse in the Mouse

(A) AMPAR currents measured at −70 mV in P5 and P9 mice (average of 20 sweeps). NMDAR currents are measured at +40 mV in the presence of 10 μM NBQX and 50 μM picrotoxin. (B) Summary graph of many such measurements in young (P3–P6; n = 17; AMPAR/NMDAR median = 0.27 ± 0.12) and older mice (P8–P11; n = 14; AMPAR/NMDAR median = 1.36 ± 0.58), showing a significant increase in the AMPA/NMDA receptor-medicated currents ($p < 0.01$, Mann-Whitney rank sum test). Box plots show the median, 10th, 25th, 75th, and 90th percentiles as *vertical boxes* with *error bars.* Note log scale of the ordinate. (C) Example traces (average of 10 sweeps) show that NMDAR currents are significantly longer lasting at P5 (top) than at P10 (middle). Traces are rescaled to same amplitude for comparison in the bottom panel. (D) Example traces (average of 10 sweeps) showing decreased ifenprodil sensitivity with age. (E) Summary measurements of NMDAR mediated current kinetics at thalamocortical synapses. At P9–P11 (n = 14; 183 ± 22 ms), currents are significantly faster than at P3–P4 or P5–P6 ($p < 0.01$; n = 8 at P3–P4, 307 ± 35 ms; n = 10 at P5–P6, 283 ± 39 ms). (F) Summary of ifenprodil sensitivity data for different age groups, showing a progressive decrease in ifenprodil sensitivity (P3–P4, n = 9, 81% ± 3%; P5–P6, n = 13, 67% ± 4%; P9–P11, n = 15, 32% ± 5%). Statistically significant difference for all ages ($p < 0.05$ between P3–P4 and P5–P6; $p < 0.01$ between P9–P11 and both P5–P6 and P3–P4).
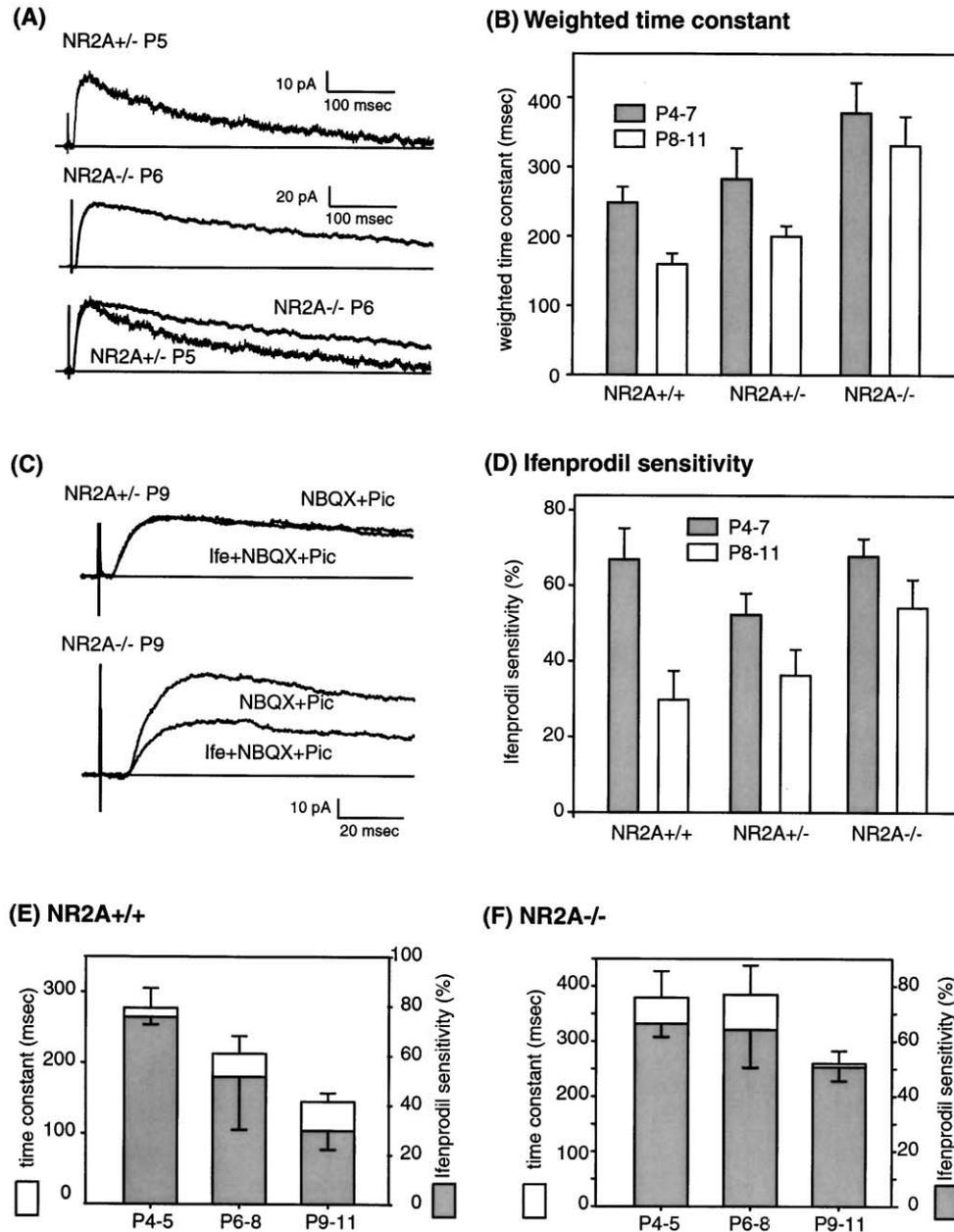
Figure 3. Thalamocortical Synaptic Response in NR2A Mutant Mice

(A) Example traces of NMDAR currents (average of ten sweeps) from $NR2A^{+/-}$ and $NR2A^{-/-}$ mice. Bottom panel shows the two current averages rescaled to the same amplitude, revealing the slower NMDAR kinetics in $NR2A^{-/-}$ mice. (B) Weighted time constant for the NMDAR current at P4–P7 (gray bars) in $NR2A^{-/-}$ mice (378 ± 43 ms; n = 10) is significantly longer than $NR2A^{+/+}$ littermates ($NR2A^{+/+}$, 249 ± 23 ms; n = 12; p < 0.01), with $NR2A^{+/-}$ littermates midway between (283 ± 44 ms; n = 8). At P8–P11 (open bars), the weighted time constant in $NR2A^{-/-}$ mice (331 ± 42 ms) is significantly longer than $NR2A^{+/+}$ (160 ± 15 ms; n = 11; p < 0.01) or $NR2A^{+/-}$ (200 ± 15 ms; n = 12; p < 0.01) littermates. (C) Example traces of isolated NMDAR currents (+40 mV) and the effects of the NR2B antagonist ifenprodil (3 μM) in $NR2A^{+/-}$ and $NR2A^{-/-}$ mice. (D) Summary of ifenprodil sensitivity data. At P4–P7, when NR2A subunits have only a minor contribution to NMDAR currents, there is no statistically significant difference between the $NR2A^{-/-}$ (68% ± 5%; n = 10) and either $NR2A^{+/-}$ (52% ± 6%; n = 6) or $NR2A^{+/+}$ (67% ± 8%; n = 11; p > 0.5) littermates. At P8–P11, the $NR2A^{-/-}$ mice remain very sensitive to ifenprodil (54% ± 7%; n = 7), significantly more so than $NR2A^{+/+}$ mice (30% ± 8%; n = 6; p < 0.05), with $NR2A^{+/-}$ (36% ± 7%; n = 7) midway between. (E) Redisplay of the time constant and ifenprodil sensitivity data in $NR2A^{+/+}$ (E) and $NR2A^{-/-}$ mice (F) to facilitate a direct comparison between changes in ifenprodil sensitivity and time constant. Note (E) the decrease in ifenprodil sensitivity (gray bars) with age and a parallel, but quantitatively smaller, shortening of the time constant (open bars) in the $NR2A^{+/+}$ mice. (F) In $NR2A^{-/-}$ mice, both the ifenprodil sensitivity and time constant remain high, though there is a small decrease in both at P9–P11 that fails to reach statistical significance.

et al., 1999). We report here a correlation between normal developmental changes in the NR2A contribution to thalamocortical synaptic response, NMDAR current

kinetics, and the end of the critical period for both barrel map plasticity and synaptic plasticity. Furthermore, we also show that LTP is blocked by the NR2B antagonist

ifenprodil (Figure 1), suggesting a subunit-specific regulation of thalamocortical synaptic plasticity. This supports the widely advanced hypothesis that regulation of NMDAR subunit expression, due either to changes in NMDA current kinetics or some other biochemical process associated with the incorporation of the NR2A subunit into the NMDAR, may act to close the critical period plasticity window in cortex. If this hypothesis is correct, the critical period for both synaptic plasticity and barrel map plasticity should be extended in *NR2A*$^{-/-}$ mice relative to *NR2A*$^{+/+}$ controls.

We first examined whether LTP can be induced in *NR2A*$^{-/-}$ mice before the end of the critical period, as in wild-type mice (Figure 1). Thalamocortical synaptic plasticity was measured in *NR2A*$^{-/-}$ mice (Figures 4A–4D) with a pairing protocol, as before (Figure 1). Littermate controls were used to quantitatively compare the extent of LTP between *NR2A*$^{-/-}$, *NR2A*$^{+/-}$, and *NR2A*$^{+/+}$ mice while remaining blind to their genotype. The extent of LTP induced at thalamocortical synapses in *NR2A*$^{-/-}$ mice (33% ± 13%; n = 9) at P3–P7 was not different from the LTP induced in *NR2A*$^{+/-}$ (34% ± 9%; n = 12) and *NR2A*$^{+/+}$ littermates of the same age (39% ± 6%; n = 13; p > 0.6 for all differences). The magnitude of LTP in the *NR2A*$^{+/+}$ mice was somewhat smaller than reported earlier in wild-type mice (Figure 1C), though the difference was not statistically significant and likely due to several factors, including the older average age of the *NR2A*$^{+/+}$ mice (most were P5–P7), the mixed background of the wild-type mice (C57/BL6 and FVB), and the necessity to sometimes accept more marginal recordings in the NR2A litters in order to prevent inadvertent biasing of the sample population. The absence of a difference in the magnitude of LTP in the *NR2A*$^{-/-}$ mice relative to their littermate controls suggests that the NR2A mutation had no effect on critical period thalamocortical synaptic plasticity.

Significant functional expression of NR2A currents is apparent in *NR2A*$^{+/+}$ mice at the end of the first postnatal week (Figure 3). In *NR2A*$^{-/-}$ mice, the incorporation of NR2A into the NMDAR that normally occurs at the end of the first postnatal week is not possible. Nonetheless, LTP cannot be induced beyond the critical period (P8–P11) in *NR2A*$^{-/-}$ mice (−5% ± 5%; n = 8), even with their slow NMDA currents (Figures 4E–4H). Similarly, it was difficult to induce LTP in *NR2A*$^{+/+}$ (9% ± 13%; n = 8) and *NR2A*$^{+/-}$ littermates at this late age (2% ± 6%; n = 13), as was observed earlier (Figure 1). Thus, the critical period for thalamocortical LTP remains unchanged in NR2A mutant mice. These data indicate that developmental regulation of the expression of the NR2A subunit is not necessary for closing the critical period for thalamocortical synaptic plasticity in mice.

AMPAR/NMDAR in *NR2A*$^{-/-}$ Mice

One explanation for why LTP in the *NR2A*$^{-/-}$ mice was difficult to induce after the critical period is that the *NR2A*$^{-/-}$ mutation could have greatly reduced the total number of NMDARs, resulting in smaller evoked NMDAR currents. If true, this should be manifested as an increase in the AMPAR/NMDAR current ratio in the *NR2A*$^{-/-}$ mice. We looked for changes in the relative amplitude of the NMDA and AMPA currents (AMPAR/
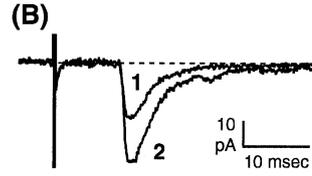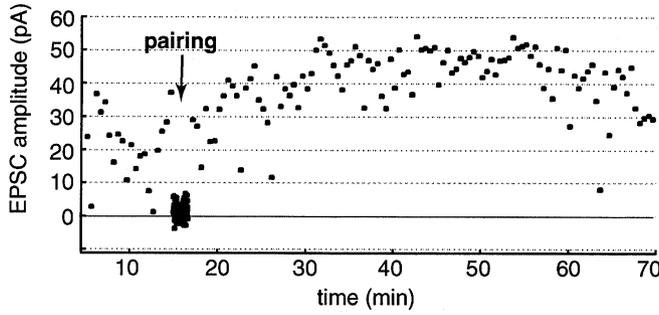
NMDAR) in the *NR2A*$^{-/-}$ mice in comparison to littermate controls (Figures 5A and 5B). No difference was detected (P8–P11, *NR2A*$^{+/+}$ = 0.73 ± 0.951, n = 7; *NR2A*$^{+/-}$ = 1.32 ± 0.59, n = 8; *NR2A*$^{-/-}$ = 0.32 ± 1.05, n = 5; p = 0.812, Kruskal-Wallis analysis of variance on ranks) (Figure 5B). Similar results were found for younger mice (P3–P6, data not shown), when no difference between *NR2A*$^{-/-}$ and *NR2A*$^{+/+}$ mice is expected.

Since there was no evidence of a decrease in NMDA currents (increase in AMPA/NMDA ratio) in the barrel cortex of the *NR2A*$^{-/-}$ mice (Figures 5A and 5B), we used quantitative Western analysis to examine if a compensatory increase could be detected in the level of NR2B subunit expression (Figures 5C and 5D). No difference was found in the levels of NR2B, NR1, or GluR1 protein in the barrel cortex of *NR2A*$^{-/-}$, *NR2A*$^{+/-}$, or *NR2A*$^{+/+}$ mice at P10. Quantitative comparisons were performed for both the absolute level of expression (example blot shown in Figure 5C) and relative levels of expression using actin protein as a standard (summary quantification in Figure 5D). This is consistent with a previous report by Sakimura et al. (1995) that no up regulation of NR2B expression occurs in *NR2A*$^{-/-}$ mice. Sakimura et al. (1995) also noted an increase in the evoked AMPA/NMDA current ratio at hippocampal synapses in adult *NR2A*$^{-/-}$ mice relative to *NR2A*$^{+/+}$ controls. Our failure to detect a difference in AMPA/NMDA currents in the neonatal *NR2A*$^{-/-}$ mice is likely age related because significant NR2B expression persists in the cortex and hippocampus well past P10 but is small in adults. In sum, the effects of the NR2A mutation on the amplitude of the evoked NMDA current is quite muted at this age due to the high abundance of NR2B receptors (Monyer et al., 1994), though we did detect a large effect on NMDAR current kinetics and ifenprodil sensitivity (Figure 3).
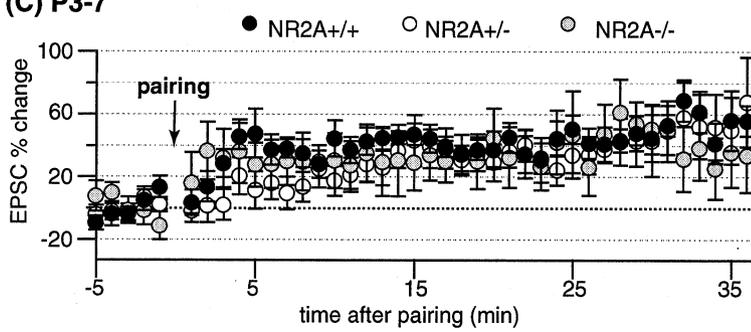
Barrel Map Plasticity Unchanged in *NR2A*$^{-/-}$ Mice

Depriving rodents of sensory experience by removing the C-row of whiskers at a young age induces a filling-in of the cortical barrel map. We examined this anatomical map plasticity in the *NR2A*$^{-/-}$ mice to determine whether the critical period for barrel plasticity is prolonged in the absence of NR2A incorporation into the NMDAR. Cytochrome oxidase (CO)-stained tangential sections through layer IV of barrel cortex show evidence of filling-in due to neonatal whisker deprivation in all the whisker-deprived animals, regardless of genotype (Figures 6A–6C). In order to quantitatively examine barrel plasticity in *NR2A*$^{-/-}$ mice, we first lesioned the C-row of whiskers at P1 in *NR2A*$^{-/-}$, *NR2A*$^{+/-}$, and *NR2A*$^{+/+}$ littermates (Figures 6A–6C), then assayed cortical map plasticity 2 weeks later. The potency of the lesion was always confirmed with H-E staining of the whisker pads (Figure 6J). A quantitative measure of anatomical plasticity, defined as a Map Plasticity Index (MPI) (see Experimental Procedures and Figure 6K), was used to examine if any subtle plasticity differences could be detected in the *NR2A*$^{-/-}$ mice compared to *NR2A*$^{+/-}$ and *NR2A*$^{+/+}$ mice. No difference was found (*NR2A*$^{-/-}$ MPI = 0.29 ± 0.02, n = 5; *NR2A*$^{+/-}$ MPI = 0.22 ± 0.03, n = 6; *NR2A*$^{+/+}$ MPI = 0.30 ± 0.09, n = 2), confirming that normal barrel map plasticity existed in NR2A mutants due to neonatal (P1) whisker deprivation.
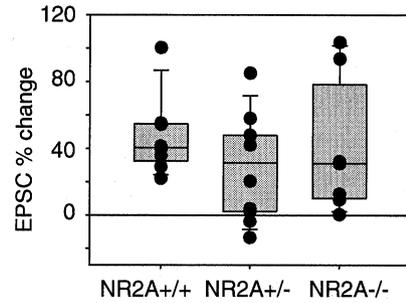
(A) NR2A-/- P3
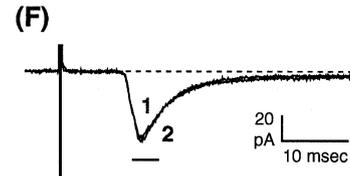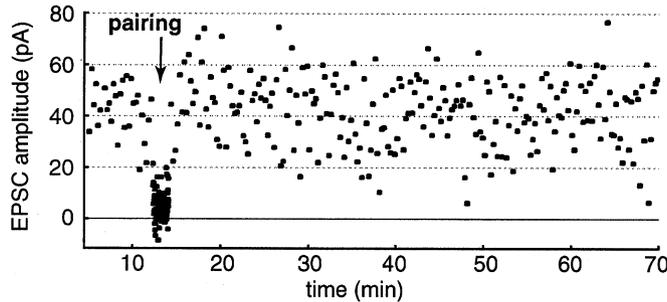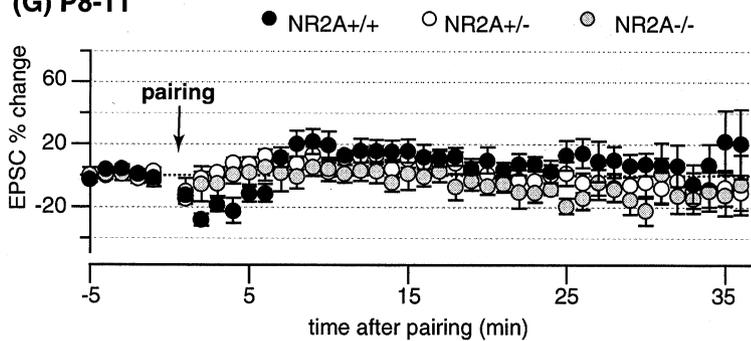
(B)

(C) P3-7

(D) P3-7

(E) NR2A-/- P8

(F)
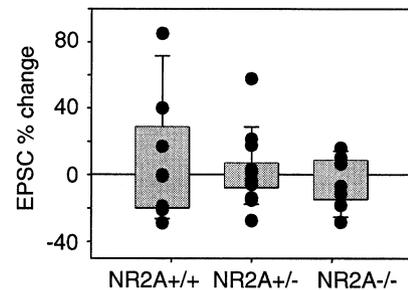
(G) P8-11

(H) P8-11

Figure 4. Normal Critical Period LTP in $NR2A^{-/-}$ Mice

(A) Example of pairing induced LTP from an $NR2A^{-/-}$ mouse at P3. (B) EPSC traces (average of 10) from before (−5–0 min) and after (15–20 min) pairing. (C) Summary graph from $NR2A^{+/-}$ (open circles, n = 12) $NR2A^{+/+}$ (n = 13, filled black circles) and $NR2A^{-/-}$ mice (n = 9, filled gray circles). (D) EPSC % change as a result of LTP pairing in $NR2A^{-/-}$ mice (n = 9; 33% ± 3%) was similar in amplitude to the $NR2A^{+/-}$ (n = 12; 34 ± 9%) and $NR2A^{+/+}$ (n = 13; 39 ± 6%) mice during the critical period (P3–P6). (E) Example of pairing effect after the critical period (P8) in $NR2A^{-/-}$ mouse. (F) Example EPSC traces before (1) and after (2) pairing (average of 20 sweeps). (G) Summary graph from older (P8–P11) $NR2A^{-/-}$ (n = 8, filled gray circles), $NR2A^{+/-}$ (n = 13, open circles) and $NR2A^{+/+}$ (n = 8, filled black circles) littermates. (H) EPSC % change 15–20 min after pairing relative to 0–5 min before pairing in older (P8–P11) mice show no LTP on average regardless of genotype ($NR2A^{-/-}$, −5% ± 5%, n = 8; $NR2A^{+/-}$, 2% ± 6%, n = 13; $NR2A^{+/+}$, 9% ± 13%, n = 8). Box plots show the median, 10th, 25th, 75th, and 90th percentiles as *vertical boxes* with *error bars*.

(A) AMPAR/NMDAR

(B) Summary of P8-11 AMPAR/NMDAR

(C) Western Analysis (P10)
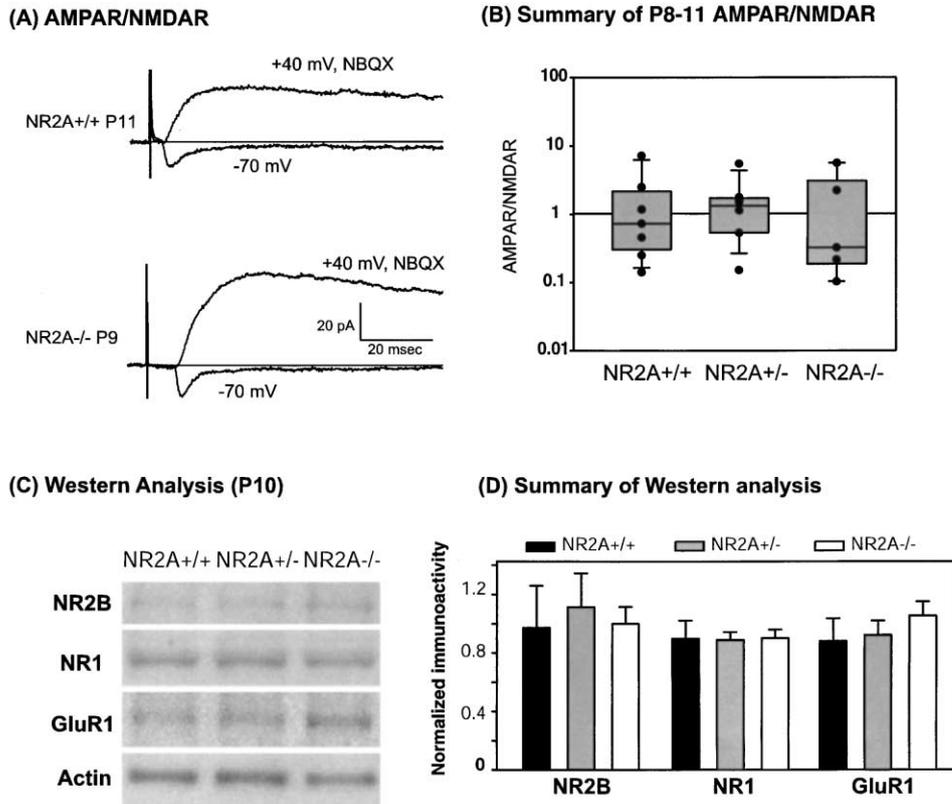
(D) Summary of Western analysis

Figure 5. AMPAR/NMDAR Current Ratio Is Unchanged in Neonatal NR2A Mutant Mice

(A) Example traces of AMPAR and NMDAR currents from $NR2A^{+/+}$ and $NR2A^{-/-}$ mice. (B) Summary data of AMPAR/NMDAR current ratio in $NR2A^{+/+}$ (0.73 ± 0.95; n = 7), $NR2A^{+/-}$ (1.32 ± 0.59; n = 8) and $NR2A^{-/-}$ (0.32 ± 1.05; n = 5) littermates. No difference between genotypes was found (p = 0.812, Kruskal-Wallis analysis of variance on ranks). Vertical box plot displays the median, 10%, 25%, 75%, and, 90% as *vertical boxes* with *error bars.* Note the log scale of the ordinate. (C) Western blots of P10 barrel cortex using antibodies against NR2B, NR1, GluR1, and Actin. (D) Summary quantification of Western blots, using I-125 phosphoimaging and densitometric quantification of ECL bands. No difference between genotypes was detected, either in the absolute level of protein expression or in the ratio of normalized expression relative to the abundant cytoskeletal protein, Actin. Normalized immunoreactivity of NRB/Actin was 0.97 ± 0.28 for n = 4 $NR2A^{+/+}$ mice, 1.11 ± 0.23 for n = 4 $NR2A^{+/-}$ mice, and 1.00 ± 0.12 for n = 5 $NR2A^{-/-}$ mice; p > 0.65 for all comparisons. Normalized immunoreactivity of NR1/Actin was 0.89 ± 0.12 for n = 5 $NR2A^{+/+}$ mice, 0.89 ± 0.05 for n = 6 $NR2A^{+/-}$ mice, and 0.90 ± 0.06 for n = 6 $NR2A^{-/-}$ mice; p > 0.88 for all comparisons. Normalized immunoreactivity of GluR1/Actin was 0.88 ± 0.15 for n = 6 $NR2A^{+/+}$ mice, 0.92 ± 0.10 for n = 6 $NR2A^{+/-}$ mice, and 1.05 ± 0.10 for n = 6 $NR2A^{-/-}$ mice, p > 0.37 for all comparisons.

Next, we lesioned the C-row of whiskers at P5 near the end of the critical period for anatomical barrel map plasticity to examine whether the critical period for map plasticity is prolonged in $NR2A^{-/-}$ mice (Figures 6D–6F). Lesions at P5 resulted in CO barrel patterns in $NR2A^{-/-}$ mice that were indistinguishable from $NR2A^{+/-}$ and $NR2A^{+/+}$ littermates ($NR2A^{-/-}$ MPI = 0.87 ± 0.05, n = 5; $NR2A^{+/-}$ MPI = 0.98 ± 0.06, n = 2; $NR2A^{+/+}$ MPI = 0.87 ± 0.01, n = 3) (Figure 6K). Recently, whisker lesions in a cortex-specific NR1 mutant, as well as in PLC-β1 and mGluR5 mutants, were shown to have a greater effect on barrel cytoarchitectonics measured with Nissl-stained sections of layer IV neurons than on CO barrels, which may preferentially label thalamocortical afferents (Iwasato et al., 2000; Hannan et al., 2001). Because of this distinction, we also quantitatively examined barrel cytoarchitectonic plasticity in Nissl-stained sections through layer IV of the $NR2A^{-/-}$ mice, but again, no plasticity difference was observed ($NR2A^{-/-}$ MPI = 0.99 ± 0.05, n = 3;

$NR2A^{+/-}$ MPI = 0.98 ± 0.05, n = 6; $NR2A^{+/+}$ MPI = 0.93 ± 0.02, n = 6) (Figures 6G–6I and 6K).

In sum, no difference was detected in the degree of filling-in of layer IV barrels in $NR2A^{-/-}$, $NR2A^{+/-}$, and $NR2A^{+/+}$ littermates with either CO histochemistry or Nissl-stained sections (Figure 6) either after lesions at P1 or at P5. This suggests that $NR2A^{-/-}$ mice have normal barrel map plasticity and that the critical period for anatomical plasticity, like synaptic plasticity, is not affected by the NR2A mutation.

Discussion

Cortical map formation requires the accurate targeting, synaptogenesis, elaboration, and refinement of thalamic afferents to the cortex. We present evidence concerning several crucial aspects of the process of cortical map development at the thalamocortical synapse in mouse barrel cortex. First, we showed that there is an increase
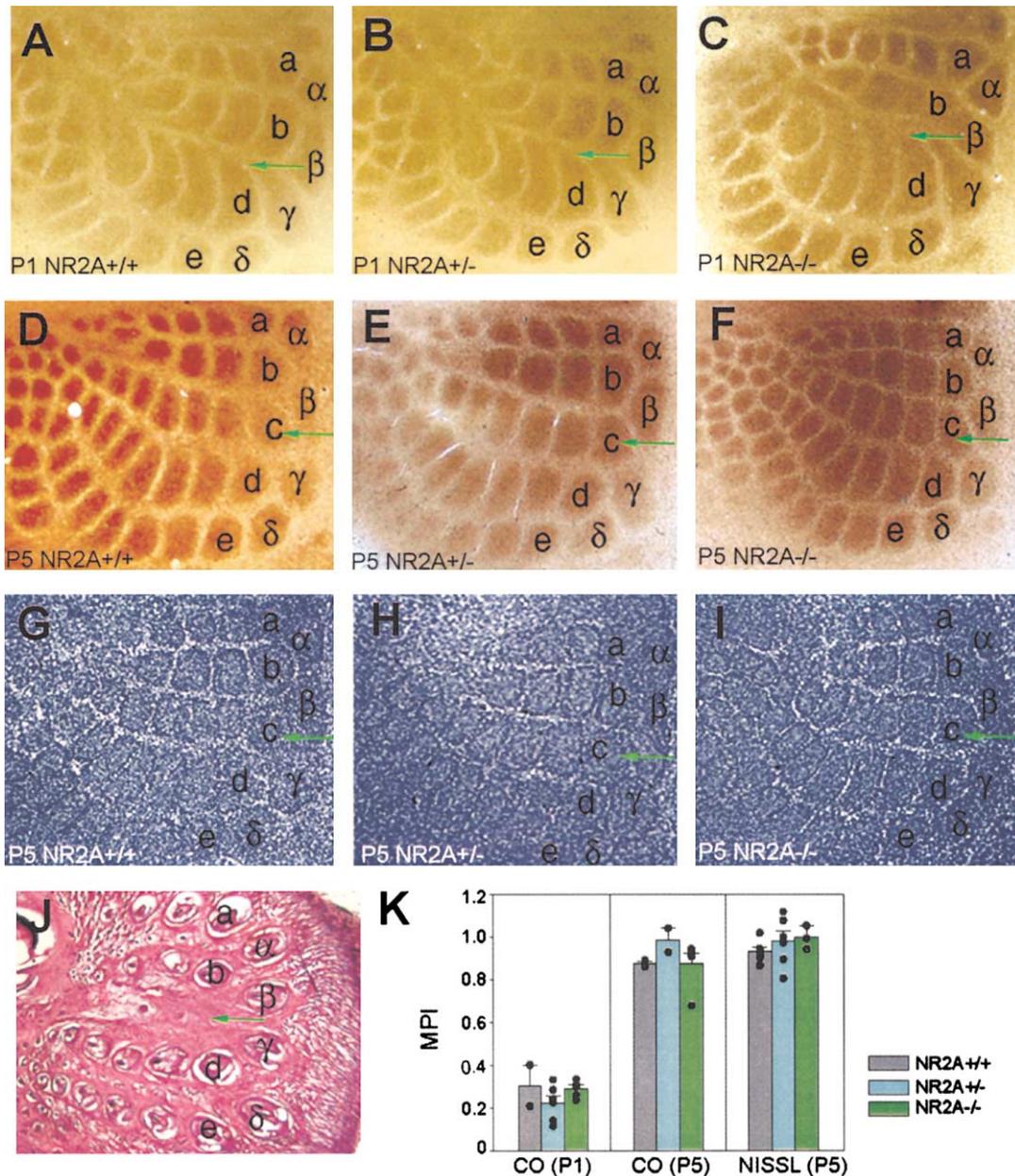
Figure 6. Critical Period for Barrel Map Anatomical Plasticity Is Unchanged in NR2A Mutant Mice

(A–C) CO stain reveals barrel map plasticity from C-row whisker lesions at P1 (note missing C-row at green arrow) in $NR2A^{+/+}$ (A), $NR2A^{+/-}$ (B), and $NR2A^{-/-}$ mice. (D–F) Example CO barrel patterns after C-row deprivation in $NR2A^{+/+}$ (D), $NR2A^{+/-}$ (E), and $NR2A^{-/-}$ (F) mice near the end of the critical period (P5). (G–I) Nissl stain shows intact cortical cytoarchitecture in $NR2A^{+/+}$ (G), $NR2A^{+/-}$ (H), and $NR2A^{-/-}$ (I) mice after C-row deprivation at P5. (J) H-E staining of hair follicles on the snout confirms successful C-row lesions (follicles missing at green arrow). (K) Summary quantification of barrel map plasticity using the MPI (see Experimental Procedures). CO patterns for P1-deprived mice show significant plasticity (expansion of barrels neighboring the C-row) in $NR2A^{+/+}$ (MPI = 0.30 ± 0.09; n = 2), $NR2A^{+/-}$ (MPI = 0.22 ± 0.03; n = 6), and $NR2A^{-/-}$ (MPI = 0.29 ± 0.02; n = 5) mice. Middle histograms shows a summary quantification of CO barrel map plasticity (MPI) for P5-deprived $NR2A^{+/+}$ (MPI = 0.87 ± 0.01; n = 3), $NR2A^{+/-}$ (MPI = 0.98 ± 0.06; n = 2) and $NR2A^{-/-}$ (MPI = 0.87 ± 0.05; n = 5) mice. The last set of histograms shows the summary quantification (MPI) for Nissl-stained sections from $NR2A^{+/+}$ (MPI = 0.93 ± 0.02; n = 6), $NR2A^{+/-}$ (MPI = 0.98 ± 0.05; n = 6) and $NR2A^{-/-}$ (MPI = 0.99 ± 0.05; n = 3) mice deprived at P5. No difference between the genotypes was detected with any of these measures.

in the relative contribution of the AMPAR to thalamocortical synaptic response and a change in the NMDAR kinetics from slow to fast during the first week after birth. Second, we observed a correlation between the critical period for barrel map plasticity and synaptic plasticity, similar to that previously reported (Crair and Malenka, 1995; Barth and Malenka, 2001), suggesting that thalamocortical LTP may share common signaling mechanisms with barrel map development and plasticity. Third, we showed that thalamocortical LTP requires

NR2B containing NMDARs, and the contribution of NR2A subunits to NMDAR response increases gradually near the end of the critical period, the same time during which the current kinetics of the NMDAR switches from slow to fast and thalamocortical LTP becomes difficult to elicit. Fourth, we used NR2A knockout mice to test the role of NMDAR subunit composition in regulating NMDAR current kinetics and critical period plasticity. We detected slower NMDAR kinetics and increased ifenprodil sensitivity at thalamocortical synapses of NR2A mutants, confirming the role of the NR2A subunit in accelerating NMDAR kinetics at the end of the critical period. To our surprise, however, thalamocortical synaptic plasticity and barrel map plasticity remain unchanged in the NR2A knockouts, suggesting that the regulation of NMDAR subunit composition is not responsible for closing the critical period in barrel cortex.

Developmental Changes in NMDAR Subunit Composition

We observed a shift in the subunit composition of the NMDA receptor at the thalamocortical synapse during development, from NR2B dominated to mixed NR2A and NR2B. In normal mice, NMDAR currents are progressively less sensitive to the NR2B antagonist ifenprodil with age, which reflects an increasing contribution of the NR2A subunit to thalamocortical synaptic response. In NR2A mutants though, the NMDAR currents remain maximally sensitive to ifenprodil. We believe that the normal developmental change in NMDAR subunit composition is also responsible for the observed change in kinetics of the NMDA current response, from slow to fast. This interpretation is confirmed in the $NR2A^{-/-}$ mice since they have a larger weighted time constant (slower kinetics) than $NR2A^{+/+}$ mice, which indicates that the NR2 subunit modulates NMDAR kinetics in situ. This is consistent with previous reports showing that NMDARs containing only NR2A subunits are intrinsically fast, whereas currents from NR2B receptors are slow (Flint et al., 1997; Vicini et al., 1998; Tovar and Westbrook, 1999; Tovar et al., 2000; Steigerwald et al., 2000).

A recent report provided evidence for a mismatch between the timing during development of changes in NMDAR current kinetics and changes in NMDAR subunit composition at the thalamocortical synapse (Barth and Malenka, 2001). Our data using NR2A knockout mice show definitively that NMDAR subunit composition is responsible for much of the developmental change in NMDAR current kinetics from P4–P11 (Figures 2E, 2F, 3E, and 3F). The discrepancy in this data is probably due to one or more experimental differences, including: (1) when isolating the NMDAR currents, we include the fast Ca^{2+} chelator BAPTA in our whole-cell pipette. We did this to avoid inadvertently inducing LTP (pairing) in the neuron while measuring the NMDA currents at a depolarized potential, and also to block any Ca^{2+}-mediated processes that may modify NMDA current kinetics (Umemiya et al., 2001; McBain and Mayer, 1994). (2) We used a double exponential fit of the falling phase of the NMDA current out to 600 ms from the peak to analyze the NMDAR current kinetics. We believe this gives a more reliable quantification of the slow kinetics of the NMDA current than a single exponential fit to a shorter portion of the decaying phase of the NMDA current (Barth and Malenka, 2001). (3) We analyzed the development of the NMDA current during and just after the critical period for barrel development (P3–P11). Barth and Malenka (2001) studied this process out to 1 month after birth, when continuing changes in NMDA kinetics may be mediated by mechanisms other than those described here.

In mouse superior colliculus, there is evidence for a small mismatch in the timing of developmental changes in NMDA kinetics and the upregulation of NR2A subunit expression (Shi et al., 2000). Shi et al. (2000) have argued that the susceptibility of NMDARs to calcineurin (protein phosphatase 2B)-mediated phosphorylation is responsible for some of the developmental shortening of NMDA kinetics at the retino-collicular synapse. Our data at the thalamocortical synapse is consistent with this model, since calcineurin mediated kinetic effects may act exclusively through the NR2A subunit (Umemiya et al., 2001), and additional changes in NMDA kinetics beyond those described here may also exist. However, our data clearly show that changes in NMDAR subunit composition play a major role in the developmental regulation of NMDAR current kinetics.

NR2A, Synaptic Plasticity, and Barrel Plasticity

The NMDA receptor, potentially acting through an LTP-type mechanism at developing synapses, has been repeatedly implicated in the cellular processes responsible for cortical map development, plasticity, and the control of critical period timing (Bear, 1996; Crair, 1999; Fox and Zahs, 1994; Katz and Shatz, 1996; Singer, 1995). Evidence for this comes from a diverse set of systems, including cat visual cortex (Bear et al., 1990; Kleinschmidt et al., 1987; Roberts et al., 1998; Fox et al., 1989, 1992; Roberts and Ramoa, 1999; Catalano et al., 1997), rat visual cortex (Quinlan et al., 1999a, 1999b; Nase et al., 1999; Ramoa and Prusky, 1997; Philpot et al., 2001), and the rodent somatosensory system (Iwasato et al., 1997, 2000; Kutsuwada et al., 1996; Li et al., 1994; Crair and Malenka, 1995; Feldman et al., 1998; Schlaggar et al., 1993; Rema et al., 1998; Fox et al., 1996). The weight of this evidence strongly suggests that developmental regulation of the NMDA receptor, specifically through NR2A subunit control of the NMDAR, is a key ingredient in cortical development and plasticity. Thus, it was widely hypothesized that regulation of NMDAR subunit composition may define the critical period window for cortical map plasticity.

We tested this hypothesis with NR2A loss-of-function mutant mice. To our surprise, we found that thalamocortical barrel map and synaptic plasticity in $NR2A^{-/-}$ mice, like in wild-type mice, cannot be induced past the end of the critical period. These data indicate that the developmental increase in NR2A subunit contribution to NMDAR currents that normally occurs during the first week after birth does not close the critical period window for synaptic and map plasticity in barrel cortex, since the critical period remains unchanged in $NR2A^{-/-}$ mice despite the absence of subunit regulation. Our data show that regardless of whether or not there is a coincidence between changes in NMDAR current kinetics and developmental critical periods, NR2A subunit

regulation does not play an important role in barrel cortex critical period plasticity. Current influx through the NR2B subunit of the NMDA receptor is necessary for LTP at the thalamocortical synapse in barrel cortex (Figure 1), but regulation of NMDAR subunit composition and NMDA current kinetics do not act as a developmental "gate" for barrel map and synaptic plasticity.

Recent evidence from other investigators also suggests that the developmental regulation of NMDAR kinetics and plastic critical periods may be unrelated. For instance, in the bird song system, the NMDAR has also been strongly implicated in critical period plasticity, but the developmental change in NMDAR kinetics is not coincident with the critical period (Livingston et al., 2000). Also, in the visual cortex of the ferret, a decrease in the NMDAR decay time and up-regulation of NR2A currents appear to be coincident with the onset instead of the offset of the critical period for ocular dominance plasticity (Roberts and Ramoa, 1999). These data suggest that we must look elsewhere for a mechanistic explanation for critical period plasticity windows in the developing nervous system.

One attractive alternative model is that a developmental decrease in the total quantity of NMDAR expressed at the thalamocortical synapse, rather than regulation of the NMDAR subunit composition itself, is sufficient to control the timing of the critical period. In this scenario, the specific action of the NR2B antagonist ifenprodil in blocking critical period LTP would not be due to its NR2B specificity, but rather due to the large blockade it causes in total NMDA current, which is largely NR2B mediated at this age. Also, under this model, the unchanged critical period in the $NR2A^{-/-}$ mice would potentially be explained by a developmental downregulation in NMDAR currents, which could be even more dramatic in the $NR2A^{-/-}$ mice. We do not favor this model because the electrophysiological analysis reveals a similar AMPAR/NMDAR ratio in $NR2A^{-/-}$ and $NR2A^{+/+}$ mice, and the Western analysis also suggests there is no difference in the quantity of NMDAR (NR1) expressed in the $NR2A^{-/-}$ and $NR2A^{+/+}$ mice (Figure 5). In addition, based on Western analysis, the total quantity of NMDAR expressed in barrel cortex does not appear to decrease immediately after the critical period (data not shown).

Functional plasticity in barrel cortex, usually measured with extracellular electrodes in vivo, is also dependent on NMDAR currents (Fox et al., 1996; Rema et al., 1998). It remains possible that analysis of plasticity using in vivo techniques would reveal subtle critical period plasticity deficits in the $NR2A^{-/-}$ mice that are not apparent when measured with anatomical techniques. Barrel cortex in vivo plasticity persists into the adult, and is thought to be mediated by changes in cortical-cortical connections (Fox, 1994; Wallace et al., 2001). This suggests that expression of NMDAR-mediated plasticity may be regulated on a layer-specific or even synapse-specific basis within a given region of cortex (Stern et al., 2001). It would be interesting to know if adult barrel cortex functional plasticity, like adult hippocampal plasticity (Kiyama et al., 1998), is affected by the NR2A mutation.

Critical Period Mechanisms

There are, of course, other mechanisms related to an NMDAR-mediated cellular process but distinct from direct regulation of NMDA subunit composition that may be responsible for the control of critical period timing. For example, biochemical signaling pathways involved in glutamate receptor trafficking or gating of synaptic plasticity are likely candidates for critical period control. Some hints in this regard come from considering different strains of mutant mice that lack barrel maps in somatosensory cortex. Phospholipase C-Beta 1 may mediate glutamate signaling in the barrel field, either through mGluRs or NMDARs, since Phospholipase C-Beta 1 mutant mice are barrelless (Hannan et al., 2001). Monoamine signaling has been implicated in barrel development because knockout of the MAO-A gene, which results in elevated levels of serotonin in the cortex, also results in a barrelless phenotype (Cases et al., 1996), though serotonin receptor knockout mice apparently have normal barrels (Saudou et al., 1994). Another interesting candidate is the cAMP-signaling pathway, since adenylyl cyclase 1 (AC1) mutants are also barrelless (Abdel-Majid et al., 1998; Welker et al., 1996). cAMP signaling in barrel development may be acting through protein kinase A (PKA), which is known to be important for gating synaptic plasticity and controlling AMPAR trafficking in the hippocampus (Blitzer et al., 1995, 1998; Ehlers, 2000), and mice lacking the α and delta isoforms of the cAMP response element binding protein (CREB) have impaired barrel map plasticity (Glazewski et al., 1999).

Recently, an important role for GABA-mediated inhibition in critical period plasticity in mouse visual cortex has been highlighted (Fagiolini and Hensch, 2000; Komatsu, 1994). In this model, the onset of critical period plasticity corresponds to the time when inhibitory synapses mature and synapses begin to be consolidated. We think inhibition is less likely to be important in barrel cortex critical period plasticity because GABAergic synapses are very immature and not inhibitory at the peak of the critical period for barrel plasticity (Agmon and O'Dowd, 1992; Agmon et al., 1996), and the development of inhibitory synapses in somatosensory cortex extends for weeks past the end of the critical period for barrel map plasticity (Micheva and Beaulieu, 1996). Ultimately, the combined use of molecular genetic tools with cellular, functional, and anatomical analysis is a very promising approach to unraveling the mechanisms responsible for cortical map formation and plasticity, questions of well-recognized and long-standing interest and import.

Experimental Procedures

Animals
Data on the wild-type developmental profile of the thalamocortical synapse (Figures 1 and 2) were derived from a mixture of both C57BL/6 and FVB mice (Harlan Lab). We found no difference in the physiological properties of these two strains, so their data were pooled. Mutant mice lacking the 2A subunit of the NMDA receptor (NR2A) were produced by homologous recombination by Sakimura et al. (1995). Homozygous and heterozygous NR2A mutants were used for breeding and experiments. The NR2A mutant mice have been backcrossed successively with C57BL/6 mice for more than 13 generations to yield homozygous mutant mice ($NR2A^{-/-}$) with a 99.99% pure C57BL/6 genetic background. All experimentation and analysis was done blind to the genotype of the animal, allowing us

to use littermate controls from homozygous, heterozygous, or wild-type parents throughout. Genotypes were determined by genomic PCR from tail clippings following the protocol described in Tovar et al. (2000). Two sets of a PCR primer mixture were used to determine the genotype of each animal. Primer mix 1 contains primer 1, 2, and 3, while primer mix 2 contains primer 1, 2, and 4. Primer 1: 5′-TCT GGGGCCTGGTCTTCAACAATTCTGTGC-3′; primer 2: 5′-GCCTGCTTG CCGAATATCATGGTGGAAAAT-3′; primer 3: 5′-CCCGTTAGCCCGTTG AGTCACCCCT-3′; and primer 4: 5′-ATTCTTTGATAAATATGCAATGTAT GGGGG-3′. Animals were treated in compliance with the U.S. Department of Health and Human Services and Baylor College of Medicine guidelines.

Electrophysiology
Thalamocortical slices were prepared from P0 to P12 mouse pups (day of birth is defined as P0) as previously described (Agmon and Connors, 1991; Crair and Malenka, 1995). Briefly, pups were anesthetized with Isoflurane and decapitated. The brains were rapidly removed and submerged in ice-cold extracellular Ringers solution (composition in mM: NaCl, 124; KCl, 5; $CaCl_2$, 2; $MgSO_4$, 1.3; NaH_2PO_4, 1.25; $NaHCO_3$, 26; and glucose, 11, saturated with 95% O_2/5% CO_2). Slices (400 μm) were cut on a vibratome (Leica VT100S) at an angle of 50° from the midsagittal plane and 0° (P0–P10) or 10° (P11–P12) from the coronal plane, and then transferred to a room temperature submerged recovery chamber.

After 2–5 hr of recovery, slices were placed in a recording chamber on the stage of an Axioskop 2FS microscope (Zeiss) equipped with infrared DIC optics for visualized whole-cell patch clamp recording. Excitatory postsynaptic currents (EPSCs) were recorded from layer IV neurons in the somatosensory barrel cortex by whole-cell voltage clamp recordings with an Axopatch 1D (Axon Instruments, CA). Orthodromic stimuli of 30–300 μA were applied for 0.1 ms at 10–30 s intervals through bipolar sharpened and insulated stainless steel microelectrodes placed in the ventrobasal thalamus (VB). Recording electrodes (2–5 MΩ) for whole-cell recording contained (in mM): cesium gluconate, 99.88; CsCl, 17.5; NaOH, 0.7; HEPES, 10; EGTA, 0.2; Mg-ATP, 4; GTP, 0.3; and phosphocreatine, 7; (pH 7.2); 280–300 mOsmol. Cells were held at −70 mV to record the EPSC, except where otherwise indicated. EPSCs were accepted as monosynaptic if they exhibited a short, constant latency that did not change with either increasing stimulation intensity or increased stimulation rate. LTP was induced by holding the cell at −10 mV while simultaneously pairing with 100 1 Hz stimuli (Crair and Malenka, 1995). When measuring NMDA currents (AMPA/NMDA ratio, NMDA time constant, and ifenprodil sensitivity), BAPTA (10 mM) was added in the internal solution of the electrode to prevent inadvertent LTP of the NMDA response. Data was collected and analyzed on-line using a computer driven acquisition system (PC's with National Instrument AD boards) and software under the Igor (Wavemetrics) programming environment. Data was acquired at a sampling rate of 10 kHz and filtered at 5 kHz. Fiber volley amplitude in the internal capsule was used to monitor changes in the excitability of neurons and fibers in the thalamus (VB). Input resistance and series resistance were used to continuously evaluate and monitor cell health. Experiments in which the fiber volley, input resistance, or series resistance changed significantly (>10%) were discarded. Data in the text and summary graph were presented only if neurons had an input resistance >300 MΩ and synaptic response was stable with no sign of drift for at least 10 min before any manipulation.

Data Analysis
The EPSC amplitude was defined as the mean current during a fixed 3–4 ms window at the peak of the EPSC minus the mean current during a similar window immediately before the stimulus artifact. LTP magnitude (EPSC % change) was defined as the mean EPSC amplitude 15–20 min after pairing minus the mean EPSC amplitude 0–5 min before pairing all divided by the mean EPSC amplitude 0–5 min before pairing. The amplitude and time constant of currents used for measuring the AMPAR/NMDAR ratio and the NR2B/NR2A ratio were quantified from the average of 20–50 consecutive EPSCs. AMPAR currents were measured at −70 mV. NMDAR currents and time constants were measured at +40 mV in the presence of 10 μM NBQX (2,3-Dihydro-6-nitro-7-sulphamoyl-benzo(f)quinoxaline, Tocris)

and 50 μM Picrotoxin (Tocris). Ifenprodil-insensitive NMDAR currents were obtained by bath application of 3 μM ifenprodil for 20–30 min while holding the cell at +40 mV. The ifenprodil-sensitive currents are the difference of the average of 20–50 consecutive traces before and after ifenprodil treatment. The ifenprodil sensitivity is defined as the percentage of ifenprodil-sensitive current to total NMDAR-mediated current. The peak amplitude of these respective currents was used for quantifying the AMPAR/NMDAR ratio and the ifenprodil sensitivity.

The weighted time constant of decay of the NMDA current was calculated with a two-exponential fit ($A1e^{-t/\tau1} + A2e^{-t/\tau2}$) of the decaying phase of the current out to 600 ms. The value of the weighted time constant is defined as $\tau_{weighted} = \tau1 \times A1/(A1 + A2) + \tau2 \times A2/(A1 + A2)$. Unless otherwise stated, a paired or unpaired Student's t test, where appropriate, was used for all statistical comparisons, and results are presented as mean ± standard error of the mean. Vertical box plots (Figures 1D, 1H, 2B, 4D, 4H, and 5B) show the median as a horizontal line with 10%, 25%, 75%, and 90% as the edge of the vertical boxes and error bars. Histograms (Figures 2E, 2F, 3B, 3D–3F, 5D, and 6K) show mean and standard error of the mean.

Western Analysis
Somatosensory cortex was isolated from P10 mice (Strominger and Woolsey, 1987) and homogenized in buffer (0.32 M sucrose, 10 mM HEPES pH 7.4, 0.1 mM PMSF, 1 mg/l pepstatin, 1 mg/l leupeptin, and 1 mg/l aprotinin). Total protein (20 μg) for each lane was separated on 8% SDS-PAGE gels and electrophoretically transferred to nitrocellulose membranes. Immunoblotting was carried out using anti-Actin (1:250, SIGMA), GluR1 (1:200, Chemicon), NR1 (1:1000, Chemicon), and NR2B (1:200, Chemicon) antibodies and visualized with [I-125]-Protein A (1:1000 dilution; Amersham) or horseradish peroxidase-conjugated secondary antibodies (goat anti-rabbit or anti-mouse secondary antibodies). The signal was detected and quantified with either phosphoimager spectrometry (Molecular Dynamics, Sunnyvale, California) or with WEST PICO chemiluminescence reagent (Pierce) and densitometric quantification with NIH Image software (Scion Corp., Frederick, MD).

Sensory Manipulations
P0–P5 pups were anesthetized by cooling or Isoflurane vapor and then kept on ice during the entire surgical procedure. The C-row of whiskers on the left side of the face were identified under a surgical microscope and cauterized with a surgical cautery device (Hyfrecator 2000, ConMed Corp., NY). After cauterization, the pups were revived and returned to their mother, then sacrificed at P12–P14 for histology. Animals with incomplete or inappropriate lesions, as assayed with H-E staining of the whisker pad (see below), were excluded from further analysis.

Histology
For cytochrome oxidase (CO) and Nissl stains, most animals were sacrificed at P12–P14. Mice were deeply anesthetized with Isoflurane, decapitated, and the brain exposed. Barrel cortex from the right hemisphere was removed following the methods described in Strominger and Woolsey (1987), fixed for 2 hr in 4% PFA at room temperature, and cut tangentially (parallel to layer IV) on a vibratome into 50–100 μm sections and subject to CO staining, as described in Wong-Riley and Welt (1980), or Nissl staining (0.2% cresyl violet). Whisker pads of the lesioned (left) side were removed from the snout, pressed flat with glass plates, and fixed with 4% PFA for 2 days at 4°C. The tissue was then cryoprotected with 30% sucrose overnight, and serial 50 μm thick frozen sections were cut using a freezing microtome in a tangential plane and subjected to standard H-E staining to examine the hair follicles.

Quantification of Barrel Anatomical Plasticity
The width of CO stained whisker barrels corresponding to the b2, b3, c2, c3, d2, and d3 whiskers were measured using Adobe Illustrator. The ratio of the width of the C-row whisker barrels (c2 and c3) relative to the B and D-row whisker barrels (b2, b3, d2, and d3) was used to quantify the effects of neonatal whisker lesions using a Map Plasticity Index (MPI), defined as MPI = 2(c2 + c3)/(b2 + b3 + d2 +

d3). When this ratio is 1, the width of the C-row of whisker barrels is the same as the average of the B and D row of barrels. When the ratio is much less than 1, then the C-row of whisker barrels is narrower than the B- and D-row of barrels, indicating significant "filing-in" of the C-row. Because the lesions at P1 often resulted in indistinct C-row barrels, the widths of the c2 and c3 barrels were taken to be the distance between the inner edges of the b2 and d2 or b3 and d3 barrels, respectively.

References

Abdel-Majid, R.M., Leong, W.L., Schalkwyk, L.C., Smallman, D.S., Wong, S.T., Storm, D.R., Fine, A., Dobson, M.J., Guernsey, D.L., and Neumann, P.E. (1998). Loss of adenylyl cyclase I activity disrupts patterning of mouse somatosensory cortex. Nat. Genet. *19*, 289–291.

Agmon, A., and Connors, B.W. (1991). Thalamocortical responses of mouse somatosensory (barrel) cortex in vitro. Neuroscience *41*, 365–379.

Agmon, A., Hollriger, G., and O'Dowd, D.K. (1996). Functional GABAergic synaptic connection in neonatal mouse barrel cortex. J. Neurosci. *16*, 4684–4695.

Agmon, A., and O'Dowd, D.K. (1992). NMDA receptor-mediated currents are prominent in the thalamocortical synaptic response before maturation of inhibition. J. Neurophysiol. *68*, 345–349.

Barth, A.L., and Malenka, R.C. (2001). NMDAR EPSC kinetics do not regulate the critical period for LTP at thalamocortical synapses. Nat. Neurosci. *4*, 235–236.

Bear, M.F. (1996). Progress in understanding NMDA-receptor-dependent synaptic plasticity in the visual cortex. J. Physiol. Paris *90*, 223–227.

Bear, M.F., Kleinschmidt, A., Gu, Q.A., and Singer, W. (1990). Disruption of experience-dependent synaptic modifications in striate cortex by infusion of an NMDA receptor antagonist. J. Neurosci. *10*, 909–925.

Bi, G., and Poo, M. (2001). Synaptic modulation by correlated activity: Hebb's postulate revisited. Annu. Rev. Neurosci. *24*, 139–166.

Blitzer, R.D., Wong, T., Nouranifar, R., Iyengar, R., and Landau, E.M. (1995). Postsynaptic cAMP pathway gates early LTP in hippocampal CA1 region. Neuron *15*, 1403–1414.

Blitzer, R.D., Connor, J.H., Brown, G.P., Wong, T., Shenolikar, S., Iyengar, R., and Landau, E.M. (1998). Gating of CaMKII by cAMP-regulated protein phosphatase activity during LTP. Science *280*, 1940–1942.

Cao, Z., Lickey, M.E., Liu, L., Kirk, E., and Gordon, B. (2000a). Postnatal development of NR1, NR2A and NR2B immunoreactivity in the visual cortex of the rat. Brain Res. *859*, 26–37.

Cao, Z., Liu, L., Lickey, M., and Gordon, B. (2000b). Development of NR1, NR2A and NR2B mRNA in NR1 immunoreactive cells of rat visual cortex. Brain Res. *868*, 296–305.

Carmignoto, G., and Vicini, S. (1992). Activity-dependent decrease in NMDA receptor responses during development of the visual cortex. Science *258*, 1007–1011.

Cases, O., Vitalis, T., Seif, I., De Maeyer, E., Sotelo, C., and Gaspar, P. (1996). Lack of barrels in the somatosensory cortex of monoamine oxidase A-deficient mice: role of a serotonin excess during the critical period. Neuron *16*, 297–307.

Catalano, S.M., Chang, C.K., and Shatz, C.J. (1997). Activity-dependent regulation of NMDAR1 immunoreactivity in the developing visual cortex. J. Neurosci. *17*, 8376–8390.

Crair, M.C. (1999). Neuronal activity during development: permissive or instructive? Curr. Opin. Neurobiol. *9*, 88–93.

Crair, M.C., and Malenka, R.C. (1995). A critical period for long-term potentiation at thalamocortical synapses. Nature *375*, 325–328.

Ehlers, M.D. (2000). Reinsertion or degradation of AMPA receptors determined by activity-dependent endocytic sorting. Neuron *28*, 511–525.

Fagiolini, M., and Hensch, T.K. (2000). Inhibitory threshold for critical-period activation in primary visual cortex. Nature *404*, 183–186.

Feldman, D.E., Nicoll, R.A., Malenka, R.C., and Isaac, J.T. (1998). Long-term depression at thalamocortical synapses in developing rat somatosensory cortex. Neuron *21*, 347–357.

Flint, A.C., Maisch, U.S., Weishaupt, J.H., Kriegstein, A.R., and Monyer, H. (1997). NR2A subunit expression shortens NMDA receptor synaptic currents in developing neocortex. J. Neurosci. *17*, 2469–2476.

Fox, K. (1992). A critical period for experience-dependent synaptic plasticity in rat barrel cortex. J. Neurosci. *12*, 1826–1838.

Fox, K. (1994). The cortical component of experience-dependent synaptic plasticity in the rat barrel cortex. J. Neurosci. *14*, 7665–7679.

Fox, K., and Zahs, K. (1994). Critical period control in sensory cortex. Curr. Opin. Neurobiol. *4*, 112–119.

Fox, K., Sato, H., and Daw, N. (1989). The location and function of NMDA receptors in cat and kitten visual cortex. J. Neurosci. *9*, 2443–2454.

Fox, K., Daw, N., Sato, H., and Czepita, D. (1992). The effect of visual experience on development of NMDA receptor synaptic transmission in kitten visual cortex. J. Neurosci. *12*, 2672–2684.

Fox, K., Schlaggar, B.L., Glazewski, S., and O'Leary, D.D. (1996). Glutamate receptor blockade at cortical synapses disrupts development of thalamocortical and columnar organization in somatosensory cortex. Proc. Natl. Acad. Sci. USA *93*, 5584–5589.

Gil, Z., Connors, B.W., and Amitai, Y. (1999). Efficacy of thalamocortical and intracortical synaptic connections: quanta, innervation, and reliability. Neuron *23*, 385–397.

Glazewski, S., Barth, A.L., Wallace, H., McKenna, M., Silva, A., and Fox, K. (1999). Impaired experience-dependent plasticity in barrel cortex of mice lacing the alpha and delta isoforms of CREB, Cereb. Cortex *9*, 249–256.

Gustafsson, B., Wigstrom, H., Abraham, W.C., and Huang, Y.Y. (1987). Long-term potentiation in the hippocampus using depolarizing current pulses as the conditioning stimulus to single volley synaptic potentials. J. Neurosci. *7*, 774–780.

Hannan, A.J., Blakemore, C., Katsnelson, A., Vitalis, T., Huber, K.M., Bear, M., Roder, J., Kim, D., Shin, H.-S., and Kind, P.C. (2001). PLC-β1, activated via mGluRs, mediates activity-dependent differentiation in cerebral cortex. Nat. Neurosci. *4*, 282–288.

Hestrin, S. (1992). Developmental regulation of NMDA receptor-mediated synaptic currents at a central synapse. Nature *357*, 686–689.

Hoffmann, H., Gremme, T., Hatt, H., and Gottmann, K. (2000). Synaptic activity-dependent developmental regulation of NMDA receptor subunit expression in cultured neocortical neurons. J. Neurochem. *75*, 1590–1599.

Hubel, D.H., and Wiesel, T.N. (1977). Ferrier lecture. Functional architecture of macaque monkey visual cortex. Proc. R. Soc. Lond. B Biol. Sci. *198*, 1–59.

Isaac, J.T., Crair, M.C., Nicoll, R.A., and Malenka, R.C. (1997). Silent synapses during development of thalamocortical inputs. Neuron *18*, 269–280.

Iwasato, T., Erzurumlu, R.S., Huerta, P.T., Chen, D.F., Sasaoka, T.,

Ulupinar, E., and Tonegawa, S. (1997). NMDA receptor-dependent refinement of somatotopic maps. Neuron *19*, 1201–1210.

Iwasato, T., Datwani, A., Wolf, A.M., Nishiyama, H., Taguchi, Y., Tonegawa, S., Knopfel, T., Erzurumlu, R.S., and Itohara, S. (2000). Cortex-restricted disruption of NMDAR1 impairs neuronal patterns in the barrel cortex. Nature *406*, 726–731.

Katz, L.C., and Shatz, C.J. (1996). Synaptic activity and the construction of cortical circuits. Science *274*, 1133–1138.

Kidd, F.L., and Isaac, J.T. (1999). Developmental and activity-dependent regulation of kainate receptors at thalamocortical synapses. Nature *400*, 569–573.

Kirson, E.D., and Yaari, Y. (1996). Synaptic NMDA receptors in developing mouse hippocampal neurones: functional properties and sensitivity to ifenprodil. J. Physiol. (Lond.) *497*, 437–455.

Kiyama, Y., Manabe, T., Sakumura, K., Kawakami, F., Mori, H., and Mishina, M. (1998). Increased thresholds for long-term potentiation and contextual learning in mice lacking the NMDA-type glutamate receptor ε1 subunit. J. Neurosci. *18*, 6704–6712.

Kleinschmidt, A., Bear, M.F., and Singer, W. (1987). Blockade of "NMDA" receptors disrupts experience-dependent plasticity of kitten striate cortex. Science *238*, 355–358.

Komatsu, Y. (1994). Age-dependent long-term potentiation of inhibitory synaptic transmission in rat visual cortex. J. Neurosci. *14*, 6488–6499.

Kutsuwada, T., Sakimura, K., Manabe, T., Takayama, C., Katakura, N., Kushiya, E., Natsume, R., Watanabe, M., Inoue, Y., Yagi, T., et al. (1996). Impairment of suckling response, trigeminal neuronal pattern formation, and hippocampal LTD in NMDA receptor epsilon 2 subunit mutant mice. Neuron *16*, 333–344.

Li, Y., Erzurumlu, R.S., Chen, C., Jhaveri, S., and Tonegawa, S. (1994). Whisker-related neuronal patterns fail to develop in the trigeminal brainstem nuclei of NMDAR1 knockout mice. Cell *76*, 427–437.

Livingston, F.S., White, S.A., and Mooney, R. (2000). Slow NMDA-EPSCs at synapses critical for song development are not required for song learning in zebra finches. Nat. Neurosci. *3*, 482–488.

Malenka, R.C., and Nicoll, R.A. (1993). NMDA-receptor-dependent synaptic plasticity: multiple forms and mechanisms. Trends Neurosci. *16*, 521–527.

McBain, C.J., and Mayer, M.L. (1994). N-methyl-D-aspartic acid receptor structure and function. Physiol. Rev. *74*, 723–760.

Micheva, K.D., and Beaulieu, C. (1996). Quantitative aspects of synaptogenesis in the rat barrel field cortex with special reference to GABA circuitry. J. Comp. Neurol. *373*, 340–354.

Monyer, H., Burnashev, N., Laurie, D.J., Sakmann, B., and Seeburg, P.H. (1994). Developmental and regional expression in the rat brain and functional properties of four NMDA receptors. Neuron *12*, 529–540.

Mountcastle, V.B. (1957). Modality and Topographic Properties of Single Neurons of Cat's Somatic Sensory Cortex. J. Neurophysiol. *20*, 408–432.

Nase, G., Weishaupt, J., Stern, P., Singer, W., and Monyer, H. (1999). Genetic and epigenetic regulation of NMDA receptor expression in the rat visual cortex. Eur. J. Neurosci. *11*, 4320–4326.

Philpot, B.D., Sekhar, A.K., Xhouval, H.Z., and Bear, M.F. (2001). Visual Experience and Deprivation Bidirectionally Modify the Composition and Function of NMDA Receptors in Visual Cortex. Neuron *29*, 157–169.

Quinlan, E.M., Olstein, D.H., and Bear, M.F. (1999a). Bidirectional, experience-dependent regulation of N-methyl-D-aspartate receptor subunit composition in the rat visual cortex during postnatal development. Proc. Natl. Acad. Sci. USA *96*, 12876–12880.

Quinlan, E.M., Philpot, B.D., Huganir, R.L., and Bear, M.F. (1999b). Rapid, experience-dependent expression of synaptic NMDA receptors in visual cortex in vivo. Nat. Neurosci. *2*, 352–357.

Ramoa, A.S., and Prusky, G. (1997). Retinal activity regulates developmental switches in functional properties and ifenprodil sensitivity of NMDA receptors in the lateral geniculate nucleus. Brain Res. Dev. Brain Res. *101*, 165–175.

Rema, V., Armstrong-James, M., and Ebner, F.F. (1998). Experience dependent plasticity of adult rat S1 cortex requires local NMDA receptor activation. J. Neurosci. *18*, 10196–10206.

Roberts, E.B., Meredith, M.A., and Ramoa, A.S. (1998). Suppression of NMDA receptor function using antisense DNA block ocular dominance plasticity while preserving visual responses. J. Neurophysiol. *80*, 1021–1032.

Roberts, E.B., and Ramoa, A.S. (1999). Enhanced NR2A subunit expression and decreased NMDA receptor decay time at the onset of ocular dominance plasticity in the ferret. J. Neurophysiol. *81*, 2587–2591.

Sakimura, K., Kutsuwada, T., Ito, I., Manabe, T., Takayama, C., Kushiya, E., Yagi, T., Aizawa, S., Inoue, Y., Sugiyama, H., et al. (1995). Reduced hippocampal LTP and spatial learning in mice lacking NMDA receptor epsilon 1 subunit. Nature *373*, 151–155.

Saudou, F., Amara, D.A., Dierich, A., LeMeur, M., Ramboz, S., Segu, L., Buhot, M.C., and Hen, R. (1994). Enhanced aggressive behavior in mice lacking 5–HT1B receptor. Science *265*, 1875–1878.

Scheetz, A.J., and Constantine-Paton, M. (1994). Modulation of NMDA receptor function: implications for vertebrate neural development. FASEB J. *8*, 745–752.

Schlaggar, B.L., Fox, K., and O'Leary, D.D.M. (1993). Postsynaptic control of plasticity in developing somatosensory cortex. Nature *364*, 623–626.

Schoepfer, R., Monyer, H., Sommer, B., Wisden, W., Sprengel, R., Kuner, T., Lomeli, H., Herb, A., Kohler, M., Burnashev, N., et al. (1994). Molecular biology of glutamate receptors. Prog. Neurobiol. *42*, 353–357.

Sheng, M., Cummings, J., Roldan, L.A., Jan, Y.N., and Jan, L.Y. (1994). Changing subunit composition of heteromeric NMDA receptors during development of rat cortex. Nature *368*, 144–147.

Shi, J., Townsend, M., and Constantine-Paton, M. (2000). Activity-dependent induction of tonic calcineurin activity mediates a rapid developmental downregulation of NMDA receptor currents. Neuron *28*, 103–114.

Singer, W. (1995). Development and plasticity of cortical processing architectures. Science *270*, 758–764.

Steigerwald, F., Schulz, T.W., Schenker, L.T., Kennedy, M.B., Seeburg, P.H., and Kohr, G. (2000). C-Terminal truncation of NR2A subunits impairs synaptic but not extrasynaptic localization of NMDA receptors. J. Neurosci. *20*, 4573–4581.

Stern, E.A., Maravall, M., and Svoboda, K. (2001). Rapid development and plasticity of layer 2/3 maps in rat barrel cortex in vivo. Neuron *31*, 305–315.

Strominger, R.N., and Woolsey, T.A. (1987). Templates for locating the whisker area in fresh flattened mouse and rat cortex. J. Neurosci. Methods *22*, 113–118.

Sun, L., Shipley, M.T., and Lidow, M.S. (2000). Expression of NR1, NR2AD, and NR3 Subunits of the NMDA receptor in the cerebral cortex and olfactory bulb of adult rat. Synapse *35*, 212–221.

Tang, Y.-P., Shimizu, E., Dube, G.R., Rampon, C., Kerchner, G.A., Zhuo, M., Liu, G., and Tsien, J.Z. (1999). Genetic enhancement of learning and memory in mice. Nature *401*, 63–69.

Tovar, K.R., and Westbrook, G.L. (1999). The incorporation of NMDA receptors with a distinct subunit composition at nascent hippocampal synapses in vitro. J. Neurosci. *19*, 4180–4188.

Tovar, K.R., Sprouffske, K., and Westbrook, G.L. (2000). Fast NMDA receptor-mediated synaptic currents in neurons from mice lacking the epsilon2 (NR2B) subunit. J. Neurophysiol. *83*, 616–620.

Umemiya, M., Chen, N., Raymond, L.A., and Murphy, T.H. (2001). A calcium-dependent feedback mechanism participates in shaping single NMDA miniature EPSCs. J. Neurosci. *21*, 1–9.

Vallano, M.L., Lambolez, B., Audinat, E., and Rossier, J. (1996). Neuronal activity differentially regulates NMDA receptor subunit expression in cerebellar granule cells. J. Neurosci. *16*, 631–639.

Vicini, S., Wang, J.F., Li, J.H., Zhu, W.J., Wang, Y.H., Luo, J.H., Wolfe, B.B., and Grayson, D.R. (1998). Functional and pharmacological differences between recombinant N-methyl-D-aspartate receptors. J. Neurophysiol. *79*, 555–566.

Wallace, H., Glazewski, S., Liming, K., and Fox, K. (2001). The role of cortical activity in experience-dependent potentiation and depression of sensory responses in rat barrel cortex. J. Neurosci. *21*, 3881–3894.

Wang, Y.H., Bosy, T.Z., Yasuda, R.P., Grayson, D.R., Vicini, S., Pizzorusso, T., and Wolfe, B.B. (1995). Characterization of NMDA receptor subunit specific antibodies: distribution of NR2A and NR2B receptor subunits in rat brain and ontogenic profile in the cerebellum. J. Neurochem. *65*, 176–183.

Watanabe, M., Inoue, Y., Sakimura, K., and Mishina, M. (1992). Developmental changes in distribution of NMDA receptor channel subunit mRNAs. Neuroreport *3*, 1138–1140.

Welker, E., Armstrong-James, M., Bronchti, G., Ourednik, W., Gheorghita-Baechler, F., Dubois, R., Guernsey, D.L., Van der Loos, H., and Neumann, P.E. (1996). Altered sensory processing in the somatosensory cortex of the mouse mutant barrelless. Science *271*, 1864–1867.

Wiesel, T.N., and Hubel, D.H. (1963). Single-cell responses in striate cortex of kittens deprived of vision in one eye. J. Neurophys. *26*, 1003–1017.

Williams, K. (1993). Ifenprodil discriminates subtypes of the N-methyl D-aspartate receptor: selectivity and mechanisms at recombinant heteromeric receptors. Mol. Pharmacol. *44*, 851–859.

Wong-Riley, M.T., and Welt, C. (1980). Histochemical changes in cytochrome oxidase of cortical barrels after vibrissal removal in neonatal and adult mice. Proc. Natl. Acad. Sci. USA *77*, 2333–2337.

Woolsey, T.A. (1990). Peripheral alteration and somatosensory development. In Development of Sensory Systems in Mammals, E.J. Coleman, ed. (New York: Wiley), pp. 461–516.

Zhong, J., Carrozza, D.P., Williams, K., Pritchett, D.B., and Molinoff, P.B. (1995). Expression of mRNAs encoding subunits of the NMDA receptor in developing rat brain. J. Neurochem. *64*, 531–539.